





Strong-field ionization of homonuclear diatomic molecules using orthogonally polarized two-color laser fields

D. Habibović ¹, A. Gazibegović-Busuladžić ¹, M. Busuladžić ^{1,2}, A. Čerkić¹ and D. B. Milošević ^{1,3}

¹Faculty of Science, University of Sarajevo, Zmaja od Bosne 35, 71000 Sarajevo, Bosnia and Herzegovina

²Faculty of Medicine, University of Sarajevo, Čekaluša 90, 71000 Sarajevo, Bosnia and Herzegovina

³Academy of Sciences and Arts of Bosnia and Herzegovina, Bistrik 7, 71000 Sarajevo, Bosnia and Herzegovina



(Received 3 April 2020; revised 31 May 2020; accepted 23 July 2020; published 11 August 2020)

Using the improved molecular strong-field approximation we investigate high-order above-threshold ionization (HATI) of homonuclear diatomic molecules by an orthogonally polarized two-color (OTC) laser field. The OTC field components are linearly polarized, having the relative phase φ and frequencies $r\omega$ and $s\omega$ (r and s are integers and ω is the fundamental frequency). The molecule is aligned in the laser-field polarization plane. We have found that for even values of $r + s$ the HATI spectra obey the C_2 rotational symmetry regardless of the relative phase, component intensities, and molecular orientation, while the spectra calculated for odd values of $r + s$ and for certain molecular orientations exhibit the reflection symmetry. We have also explored the symmetry transformations of the HATI spectra for a shift of the relative phase by 180° and for various values of r and s . These symmetries are illustrated by numerical examples of the HATI spectra of the N_2 molecule. For particular values of the laser-field parameters, internuclear distance, and the electron emission angle we observed minima in the ionization yield as a function of the molecular orientation angle and the photoelectron energy. These minima are well fitted with the curve obtained using a condition for the destructive interference minima which we derived for an arbitrary laser field and applied to the OTC field. The relative phase between the OTC field components can be used to control the length and shape of the HATI plateau, as well as the appearance of these destructive interference minima.

DOI: [10.1103/PhysRevA.102.023111](https://doi.org/10.1103/PhysRevA.102.023111)

I. INTRODUCTION

During the last few decades various atomic and molecular processes in a strong laser field have attracted a lot of attention. These processes can be divided into two groups: laser-induced and laser-assisted processes. Laser-induced processes are possible only in a strong laser field. Laser-assisted processes may occur also in the absence of an external field, but these processes are modified if a strong laser field is present. The focus of our paper is on the above-threshold ionization (ATI) and high-order above-threshold ionization (HATI) processes, which belong to the laser-induced processes.

A common way to describe high-order laser-induced processes is to use the so-called three-step model [1–4]. In the first step, the atom or molecule is ionized by the laser field. The second step describes the motion of the released electron in the laser field. If the electron goes directly to the detector without interacting with the parent atomic or molecular ion, the process is called ATI [5]. The liberated electron, driven by the oscillatory laser field, may return to the parent ion and elastically scatter off it before reaching the detector. This is the third step and the resulting process is called HATI. The energy spectra of the HATI process are characterized by a broad energy interval in which the photoelectron yield is practically constant; i.e., it has a plateau-like structure. This plateau region is followed by an abrupt cutoff (see, for example, review articles [6,7] and references therein). Calculation of

the (H)ATI spectra for atomic targets requires knowledge of the atomic-ground-state and the laser-field parameters. In the case of molecular targets, there are additional parameters that affect the process. The symmetry of the initial electronic state and the orientation of the molecule relative to the laser field should be taken into account.

Linearly polarized laser fields are usually used for investigation of the high-order laser-induced processes. The reason is that the liberated electron, driven by a linearly polarized laser field, can easily return to the parent ion, while in a general case of an elliptically polarized laser field this electron “misses” the parent ion (the overlap of the corresponding wave packets is very small), so that the probability of high-order processes is negligible. More recently, it has been confirmed that the high-order processes can be induced by applying more complex laser-field configurations. Such, the so-called tailored, laser fields consist of two or more field components having different frequencies and polarizations [8]. For example, a bicircular field is a superposition of two coplanar counter-rotating circularly polarized fields having different frequencies. If this field is applied in the high-order harmonic generation process, the emitted harmonics are circularly polarized [9–13]. The synthesized two-color fields are a powerful tool for control of the strong-field ionization dynamics. One can achieve a subtle control of the direct ionization and of the rescattering of photoelectrons by tuning the parameters of such two-color laser fields. One of the widely used tailored laser fields is the

orthogonally polarized two-color (OTC) laser field. This field consists of two linearly polarized components with orthogonal polarizations and commensurable frequencies. More information about high-order harmonic generation by the OTC field can be found in [14] and references therein.

In the present paper we analyze the molecular (H)ATI process driven by an OTC laser field. The OTC laser fields are often used to control the subcycle photoelectron wave packet dynamics by varying the relative phase between the laser-field components [15–18]. The OTC laser field was applied in [19] for velocity map imaging spectroscopy by using an unconventional orientation, with the polarization of the ionizing laser field perpendicular to the detector surface and the steering field parallel to it. The laser-induced tunneling was studied in [20], where a weak probe field was used to steer the tunneled electron in the lateral direction and then the effect on the attosecond light bursts emitted when the liberated electron reencounters the parent ion was monitored. The OTC-laser-field-induced electron tunneling was considered for negative ions [21] and atoms [22–37]. More recently, a streaking method for strong-field ionization by a tailored field which consists of a bicircular and a linearly polarized (orthogonal or parallel) field was proposed [38]. The temporal double-slit experiment [39] with an OTC field was realized in [40]. The control of the electron spin polarization in strong-field ionization [41] using the OTC field was proposed in [42].

There are only a small number of papers in which the ATI of molecules by an OTC field was considered. In [43] the photoelectron momentum distributions for strong-field ionization of aligned H_2^+ molecules by an OTC field of equal frequencies was investigated (this case is not of our interest here). Photoelectron momentum spectra for aligned H_2^+ molecules exposed to an ω - 2ω OTC field with the relative phase equal to zero were studied in [44]. The simulations have been performed using the two-dimensional time-dependent Schrödinger equation (TDSE), strong-field approximation (SFA), and a semiclassical electron-ensemble model. The strong-field ionization of diatomic molecules by an ω - 2ω OTC laser field was also considered in [45]. The photoelectron momentum distributions for the N_2 and O_2 molecules were calculated by solving the two-dimensional TDSE and by a semiclassical model. It was shown that these distributions are different for atoms and molecules and the dependence of the momentum distribution on the molecular orientation and on the relative phase between the two components of the ω - 2ω OTC field was explored. In Refs. [44,45] the HATI spectra, which are the main subject of our paper, were not considered. The OTC field was used to ionize and dissociate H_2 molecules in [46]. The photoelectron circular dichroism in chiral molecules exposed to the OTC field was demonstrated in [47]. It was demonstrated in [48] that the OTC laser fields can be used to achieve a stronger molecular orientation when the nanosecond laser pulses are used.

We explore the symmetries of the system consisting of a homonuclear diatomic molecule and an OTC laser field. A system possesses the M -fold rotational symmetry C_M if it is invariant under the rotation by the angle $2\pi/M$ (in radians) about the axis perpendicular to the plane of the system. Regarding the laser-field symmetry, the laser field itself possesses the dynamical symmetry which consists of

both spatial and temporal operations [49], while the Lissajous figure of this field possesses only the spatial symmetry C_M . The Lissajous figure of a linearly polarized laser field possesses the C_2 symmetry, while it possesses the C_∞ symmetry for a circularly polarized laser field [50]. The symmetry properties for the case of a counter-rotating bicircular laser field have been examined extensively for high-order harmonic generation [50–52] and for strong-field ionization of atoms [53,54] and molecules [55]. The Lissajous figure of such a field, having the frequencies $r\omega$ and $s\omega$, with r and s integers, possesses the C_{r+s} symmetry, and so do the corresponding differential ionization rates [53].

We introduced our molecular strong-field approximation (MSFA) in [56]. Using it we simulated molecular ATI experiments [57,58]. We further developed this theory in [59–61] so that it includes rescattered electrons [this is the so-called improved MSFA (IMSFA)]. The IMSFA explains the shape of the high-energy part of the electron spectra as well as the appearance of the experimentally observed two-center destructive interference minima [62–64]. In particular, the two-source two-rescattering-centers interference survives the averaging over the laser intensity distribution in the focus and has been observed in experiments with unaligned molecules [63]. Most recently, the destructive interference minima, predicted in [59], were observed in an experiment with aligned N_2 molecules [65]. Using our theory we have also simulated experiments with few-cycle laser pulses [66] and experiments with resonance-like enhancement in HATI of N_2 and O_2 molecules [67,68].

The remainder of this paper is structured as follows. The improved molecular SFA theory for diatomic molecules in an orthogonally polarized two-color laser field is briefly presented in Sec. II. A simple analytical formula for the destructive interference minima in the photoelectron high-energy spectrum is derived. Rotational and reflection symmetries of the (H)ATI spectra of homonuclear diatomic molecules for various combinations of the frequencies of the laser-field components are explored in Sec. III. The effect of the relative-phase shift by 180° on the HATI spectra is also analyzed in this section. In Sec. IV we present numerical results for the photoelectron spectra which exhibit characteristic interference minima and show that the position of these minima is in accordance with our analytical formula derived in Sec. II. Our concluding remarks and discussion are given in Sec. V. We use the atomic system of units ($\hbar = e = m_e = 4\pi\epsilon_0 = 1$).

II. THEORY

The molecular strong-field approximation was introduced in [56], further developed in [59–61], and generalized to the case of a bicircular field in [55,69]. In the MSFA the diatomic molecule is treated as a three-particle system consisting of two ionic centers and one active electron. The laser field, diatomic molecule, and emitted electron all lie in the same plane. The laser-field coordinate system is defined by the unit vectors $\hat{\mathbf{e}}_{z_L}$ and $\hat{\mathbf{e}}_{x_L}$, while the molecular coordinate system is defined by the unit vectors $\hat{\mathbf{e}}_z$ and $\hat{\mathbf{e}}_x$. The molecule is placed along the z axis of the molecular coordinate system. The angle between the z and z_L axes is denoted by θ_L . This angle describes the position of the diatomic molecule relative

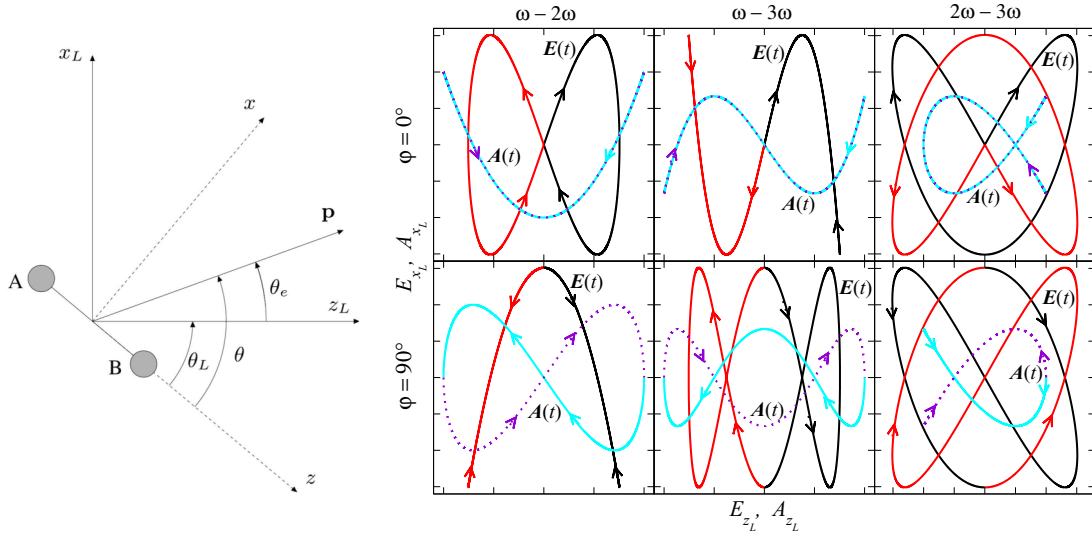


FIG. 1. Left: The coordinate systems used in the paper. Diatomic molecule is along the z axis in the zx coordinate system, while $z_L x_L$ is the coordinate system in which the laser field is defined. θ_L is the angle between the molecular axis and the z_L axis. The molecular axis and the photoelectron final momentum \mathbf{p} are in the laser-field polarization plane. The direction of the momentum \mathbf{p} is determined by the angle θ_e with respect to the z_L axis and by the angle $\theta = \theta_L + \theta_e$ with respect to the z axis. Right: Orthogonally polarized two-color laser field (the first half of a cycle, black solid line; the second half of a cycle, red solid line) and the corresponding vector potential (the first half of a cycle, cyan solid line; the second half of a cycle, violet dotted line) for $(r, s) = (1, 2), (1, 3),$ and $(2, 3)$, presented in the first, second, and third column, respectively. The relative phase is $\varphi = 0^\circ (90^\circ)$ for the upper (lower) three subpanels.

to the laser field. The y and y_L axes are perpendicular to the laser-field polarization plane. The angle between the emitted electron momentum \mathbf{p} and the z_L axis is θ_e , while the angle between the emitted electron momentum \mathbf{p} and the z axis is θ (see Fig. 1).

We suppose that the ionization occurs in the OTC laser field having the electric field vector

$$\mathbf{E}(t) = E_1 \sin(r\omega t) \hat{\mathbf{e}}_{z_L} + E_2 \sin(s\omega t + \varphi) \hat{\mathbf{e}}_{x_L}, \quad (1)$$

where $E_j = I_j^{1/2}$ and I_j are, respectively, the electric field amplitude and intensity of the j th field component ($j = 1, 2$), $r\omega$ and $s\omega$ are integer multiples of the fundamental angular frequency $\omega = 2\pi/T$, and φ is the relative phase between the field components. The unit polarization vectors along the z_L and x_L axes are related to the unit vectors along the z and x axes by the relations

$$\begin{aligned} \hat{\mathbf{e}}_{z_L} &= \cos \theta_L \hat{\mathbf{e}}_z + \sin \theta_L \hat{\mathbf{e}}_x, \\ \hat{\mathbf{e}}_{x_L} &= -\sin \theta_L \hat{\mathbf{e}}_z + \cos \theta_L \hat{\mathbf{e}}_x. \end{aligned} \quad (2)$$

For visualization of the complexity and symmetries of the considered electric field and vector potential $\mathbf{A}(t) = -\int dt \mathbf{E}(t)$, in Fig. 1 we present contours for a few (r, s) combinations of the OTC laser field and for two different relative phases. For easier tracking of the field quantities the propagation direction arrows are indicated, and also the parts of contours for the first and the second half of an optical cycle of duration T are presented with different colors. When symmetries of the field are considered, the shape of the contours is relevant, as well as the direction on the contour.

In the case of a diatomic molecule with the initial state i , having the internuclear vector \mathbf{R} , the differential ionization

rate for emission of an electron with the final momentum \mathbf{p} is

$$w_{\mathbf{R}\mathbf{p}i}(n) = 2\pi p |T_{\mathbf{R}\mathbf{p}i}(n)|^2, \quad (3)$$

where the T -matrix element $T_{\mathbf{R}\mathbf{p}i}(n)$ can be written as

$$T_{\mathbf{R}\mathbf{p}i}(n) = \int_0^T dt \frac{d}{dt} \mathcal{T}_{\mathbf{R}\mathbf{p}i}(t) e^{in\omega t}. \quad (4)$$

The energy conservation condition is $n\omega = E_{\mathbf{p}} + U_p + I_p$, where $E_{\mathbf{p}} = \mathbf{p}^2/2$, I_p is the ionization potential, and $n = n_1 r + n_2 s$ with $n_1 (n_2)$ the number of absorbed photons of frequency $r\omega (s\omega)$. $\mathcal{T}_{\mathbf{R}\mathbf{p}i}(t)$ in Eq. (4) is a T -periodic function of time

$$\mathcal{T}_{\mathbf{R}\mathbf{p}i}(t) = \mathcal{F}_{\mathbf{R}\mathbf{p}i}(t) e^{i\mathcal{U}(t)}, \quad (5)$$

with

$$\mathcal{U}(t) = \mathbf{p} \cdot \boldsymbol{\alpha}(t) + \int^t dt' \mathbf{A}^2(t')/2 - U_p t, \quad (6)$$

where $U_p = E_1^2/(2r\omega)^2 + E_2^2/(2s\omega)^2$ is the ponderomotive energy and $\boldsymbol{\alpha}(t) = \int dt \mathbf{A}(t)$. The direct electrons are described by the zeroth-order term of the MSFA. Within the dressed MSFA in the length gauge, this term is given by the matrix element [56]

$$\mathcal{F}_{\mathbf{R}\mathbf{p}i}^{(0)}(t) = \sum_{q,a} c_{qa} e^{iq\mathbf{p}\cdot\mathbf{R}/2} \langle \mathbf{p} + \mathbf{A}(t) | \mathbf{E}(t) \cdot \mathbf{r} | \psi_a \rangle. \quad (7)$$

The molecular-ground-state wave function is given by a linear combination of the Slater-type atomic orbitals $|\psi_a\rangle$. The sum over q represents the summation over the atomic centers, with $q = +1$ for the A center and $q = -1$ for the B center (see Fig. 1).

In order to describe the rescattered electrons, we also need the first-order term of the MSFA [59,60]:

$$\begin{aligned} \mathcal{F}_{\mathbf{R}\mathbf{p}i}^{(1)}(t) &= -ie^{-iS_{\mathbf{k}}(t)} \int_0^\infty d\tau \left(\frac{2\pi}{i\tau}\right)^{3/2} e^{i[S_{\mathbf{k}}(t-\tau) - I_p\tau]} \\ &\times \sum_{q'=\pm 1} V_{e\mathbf{K}}^{q'} e^{-iq'\mathbf{K}\cdot\mathbf{R}/2} \sum_{q,a} c_{qa} e^{iq\mathbf{k}\cdot\mathbf{R}/2} \\ &\times \langle \mathbf{k} + \mathbf{A}(t-\tau) | \mathbf{r} \cdot \mathbf{E}(t-\tau) | \psi_a \rangle_{\mathbf{k}=\mathbf{k}_{st}}, \quad (8) \end{aligned}$$

where $\mathbf{K} = \mathbf{k} - \mathbf{p}$, $\mathbf{k}_{st} = -\int_{t-\tau}^t dt' \mathbf{A}(t')/\tau$ is the stationary electron momentum, $\tau = t - t_0$ is the electron travel time, with t_0 the ionization time and t the rescattering time, $S_{\mathbf{k}}(t) = \int^t dt' [\mathbf{k} + \mathbf{A}(t')]^2/2$, and $V_{e\mathbf{K}}^{q'}$ is the Fourier transform of the rescattering potential at the corresponding atomic center q' . The IMSFA includes the zeroth- and the first-order term: $\mathcal{F}_{\mathbf{R}\mathbf{p}i}^{\text{IMSFA}} = \mathcal{F}_{\mathbf{R}\mathbf{p}i}^{(0)} + \mathcal{F}_{\mathbf{R}\mathbf{p}i}^{(1)}$.

The rescattering matrix element is a sum of four contributions $(q, q') = \{(1, 1), (1, -1), (-1, 1), (-1, -1)\}$. Supposing that the contributions of $V_{e\mathbf{K}}^1$ and $V_{e\mathbf{K}}^{-1}$ are approximately equal and that $c_{1a} = c_{-1a}$ (this is true for the $3\sigma_g$ highest occupied molecular orbital of the N_2 molecule considered in this paper), we obtain

$$\begin{aligned} \mathcal{F}_{\mathbf{R}\mathbf{p}i}^{(1)} &\propto \sum_{q,q'} e^{iq'\mathbf{p}\cdot\mathbf{R}/2 + i(q-q')\mathbf{k}_{st}\cdot\mathbf{R}/2} \\ &= 2\{\cos(\mathbf{p}\cdot\mathbf{R}/2) + \cos[(\mathbf{p}/2 - \mathbf{k}_{st})\cdot\mathbf{R}]\} \\ &= 4\cos(\mathbf{k}_{st}\cdot\mathbf{R}/2)\cos[(\mathbf{p} - \mathbf{k}_{st})\cdot\mathbf{R}/2]. \quad (9) \end{aligned}$$

We notice that for $c_{1a} = -c_{-1a}$ a similar formula with the factor $\cos\gamma$, $\gamma = (\mathbf{p} - \mathbf{k}_{st})\cdot\mathbf{R}/2$, can be derived, which means that even for the molecular orbitals having components of different symmetry the two-center interference which stems from the factor $\cos\gamma$ is unaffected. The interference minima appear for $\cos\gamma = 0$, i.e., for $2\gamma = (2m+1)\pi$, $m = 0, 1, 2, \dots$. Taking into account that $\mathbf{p}\cdot\mathbf{R} = Rp\cos\theta = R(p_z\cos\theta_L - p_x\sin\theta_L)$ and that $\mathbf{k}_{st}\cdot\mathbf{R} = R(k_{z,st}\cos\theta_L - k_{x,st}\sin\theta_L)$, for the destructive interference condition we obtain

$$R|(p_z - k_{z,st})\cos\theta_L - (p_x - k_{x,st})\sin\theta_L| = (2m+1)\pi. \quad (10)$$

This condition is a generalization of the interference condition derived for a linearly polarized laser field (Eq. (5) in [59]) to the case of an arbitrary laser field. We will apply this result to the OTC field in Sec. IV.

Finally, in order to illustrate strong dependence of the high-energy photoelectron spectra on the relative phase φ of the OTC field, in Fig. 2 we present the differential ionization rate of the N_2 molecule as a function of the relative phase between the $\omega-2\omega$ OTC laser field components (abscissa) and the photoelectron energy (ordinate) for a particular molecular orientation and electron emission angle (similar results are obtained for different molecular orientations and emission angles). From Fig. 2 one can see that, for a wide interval of the relative phases (from 0 to 90 degrees), the photoelectron yield is high and the cutoff can exceed $11U_p$, while for the phases in the interval from 110 to 180 degrees the cutoff is much lower (below $7U_p$) and the high-energy electrons are absent. Therefore, the relative phase can be used as an effective parameter to control the high-energy photoelectron yield in ionization by an OTC field.

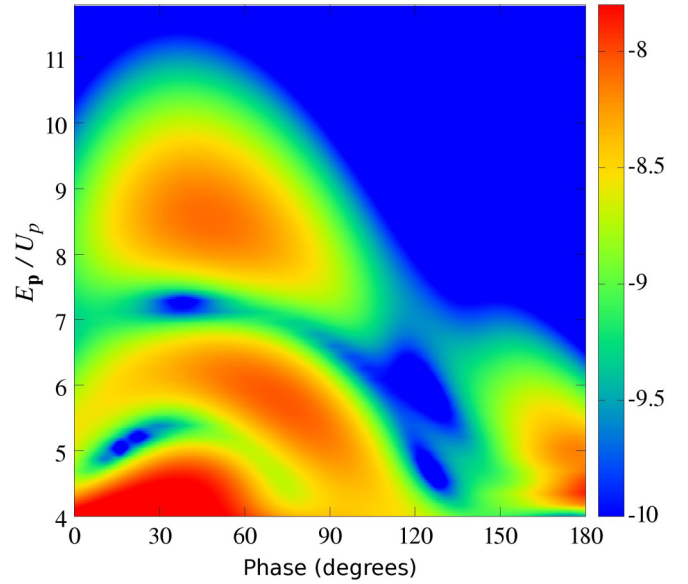


FIG. 2. Logarithm of the differential ionization rate of the N_2 molecule presented in false colors as a function of the relative phase φ of the $\omega-2\omega$ OTC laser field and the photoelectron energy E_p in units of the ponderomotive energy U_p . The intensity of the OTC field components is $I = 1.2 \times 10^{14}$ W/cm² and the fundamental wavelength is 800 nm. Molecular orientation angle is $\theta_L = 30^\circ$ and the electron emission angle is $\theta_e = -30^\circ$. The results are obtained by using the IMSFA.

III. SYMMETRIES OF THE (H)ATI SPECTRA

In all our calculations, we assume that the final electron momentum \mathbf{p} is defined in the laser-field polarization plane (i.e., in the $z_L x_L$ plane). The geometry used in our calculations is presented in Fig. 1, while the laser field is defined by Eq. (1). We also assume that the intensities of the two field components are equal ($E_1 = E_2 = E$ and $I_1 = I_2 = I$), although the presented symmetry relations are also valid for $E_1 \neq E_2$.

A. Rotation of the molecule by an angle of 180° about the y axis

The homonuclear diatomic molecules possess the C_2 symmetry. It has been shown in [55] that the corresponding differential ionization rate is invariant with respect to the transformation

$$\theta \rightarrow \theta \pm 180^\circ, \quad \theta_L \rightarrow \theta_L \pm 180^\circ, \quad \theta_e \rightarrow \theta_e. \quad (11)$$

This symmetry is generally valid, i.e., not only in the framework of the IMSFA (see Appendix A in [55]). It can be used in combination with the symmetries of the OTC field, presented in this section.

B. Dynamical symmetries of the OTC field

We consider the dynamical symmetries of the electric-field vector, having in mind that the same symmetries are also valid for the vectors $\mathbf{A}(t)$ and $\alpha(t)$. It is easy to prove that, for an arbitrary relative phase φ , the time-shift transformation $t \rightarrow t' = t + T/2$ leads to the following transformations of the electric-field components: $E_{z_L}(t') = (-1)^r E_{z_L}(t)$, $E_{x_L}(t') = (-1)^s E_{x_L}(t)$. The factor $(-1)^p$, $p = r, s$, comes from the term

$\cos(p\pi)$ that appears after the trigonometric transformations are done. For $r + s$ even, i.e., if both r and s are odd, both field components change the sign for $t \rightarrow t' = t + T/2$. This is equivalent to the rotation by 180° about the y axis, described by the rotation matrix $R_y(\pi)$. Therefore, the following symmetry relation is valid:

$$\mathbf{E}(t + T/2) = R_y(\pi)\mathbf{E}(t) = -\mathbf{E}(t), \quad r + s \text{ even}, \quad (12)$$

where we have taken into account that the laser-field polarization plane is the $z_L x_L$ plane, so that the time shift $t \rightarrow t' = t + T/2$ leads to the transformation $\mathbf{E}(t) \rightarrow -\mathbf{E}(t)$.

If $r + s$ is odd (one of the integers r and s is even and the other is odd), then for $t \rightarrow t' = t + T/2$ one of the electric-field components changes the sign while the other one remains unchanged. This corresponds to the symmetry transformation of the reflection with respect to the axis along which the electric-field component, having frequency equal to even multiple of the fundamental frequency, oscillates. These reflections are denoted by the parity operators P_{z_L} and P_{x_L} . Therefore, the time-shift transformation $t \rightarrow t' = t + T/2$ leads to

$$\mathbf{E}(t + T/2) = P_{z_L}\mathbf{E}(t), \quad r \text{ odd}, \quad (13)$$

$$\mathbf{E}(t + T/2) = P_{x_L}\mathbf{E}(t), \quad s \text{ odd}. \quad (14)$$

1. Rotational symmetry

Let us first consider the case of r and s both being odd, when the time translation $t \rightarrow t + T/2$ leads to the rotation of the field given by Eq. (12). We use the prime symbols to indicate the vectors obtained by the rotation of the original vectors by 180° about the y axis. Analogously to [53,55], we obtain that $\mathcal{F}_{\mathbf{R}\mathbf{p}i}^{\text{IMSFA}}(t)$ and $\mathcal{F}_{\mathbf{R}'\mathbf{p}'i}^{\text{IMSFA}}(t)$ are equal up to a phase factor, where the prime symbol in i means that the molecular-ground-state wave function is also rotated. In this case, the differential ionization rate (3) remains unchanged; i.e., it is invariant under the transformation

$$\theta \rightarrow \theta, \quad \theta_L \rightarrow \theta_L - 180^\circ, \quad \theta_e \rightarrow \theta_e + 180^\circ, \quad r + s \text{ even}. \quad (15)$$

This is illustrated in Fig. 3, where the HATI photoelectron spectra are presented in the momentum plane, with $p_z = \mathbf{p} \cdot \hat{\mathbf{e}}_{z_L}$ and $p_x = \mathbf{p} \cdot \hat{\mathbf{e}}_{x_L}$, for the $\omega-3\omega$ and $3\omega-5\omega$ OTC fields having the relative phase $\varphi = 0^\circ, 30^\circ, 90^\circ$, and for the molecular orientation angle $\theta_L = 0^\circ, 30^\circ, 135^\circ$. The inversion symmetry of the spectrum is visible in each of the presented cases. All HATI spectra in Fig. 3 obey the C_2 symmetry; i.e., they are invariant with respect to the transformation $\theta_e \rightarrow \theta_e + 180^\circ$. The symmetry transformation (15), i.e., $w_{\mathbf{R}'\mathbf{p}'i}(n) = w_{\mathbf{R}\mathbf{p}i}(n)$, is generally valid (compare Appendix B in [55]).

2. Reflection symmetries

We now consider the case where $r + s$ is odd. In this case, the translation in time $t \rightarrow t + T/2$ leads to the reflection of the field given by Eq. (13) for r odd and by Eq. (14) for s odd. We want to examine whether these dynamical reflection symmetries of the laser field lead to some symmetries of the HATI spectra. The invariance of the wave function of the

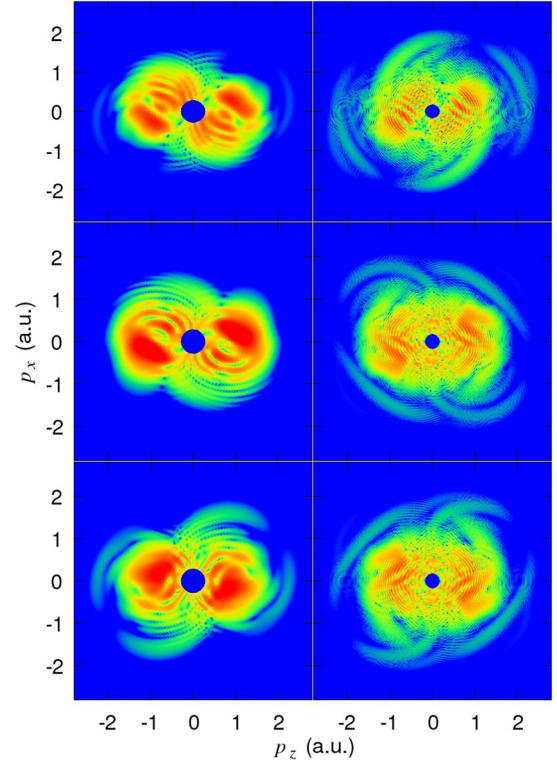


FIG. 3. Logarithm of the differential ionization rate of the N_2 molecule presented in false colors in the photoelectron momentum plane for the cases of ionization by the $\omega-3\omega$ (left column) and $3\omega-5\omega$ (right column) OTC laser fields. The intensity of the laser-field components is $I = 1.2 \times 10^{14}$ W/cm 2 . The fundamental wavelength is chosen so that $r\omega$ corresponds to 800 nm. Molecular orientations θ_L and relative phases φ are: $\theta_L = 0^\circ$ and $\varphi = 0^\circ$ (top row), $\theta_L = 135^\circ$ and $\varphi = 30^\circ$ (middle row), and $\theta_L = 30^\circ$ and $\varphi = 90^\circ$ (bottom row). The results are obtained by using the IMSFA. The false-color scale covers four orders of magnitude.

homonuclear molecule (up to a phase factor) with respect to the reflection for $\theta_L = 0^\circ, 90^\circ$ was considered in [55,69]. Let us first analyze the case where r is odd, while s is even. We denote by the double primes the vectors obtained by the reflection with respect to the $x_L y_L$ plane, e.g., $\mathbf{p}'' = P_{z_L}\mathbf{p}$, $\mathbf{R}'' = P_{z_L}\mathbf{R}$. Taking into account that $\mathbf{E}''(t) = P_{z_L}\mathbf{E}(t) = \mathbf{E}(t + T/2)$ [see Eq. (13)] and analogously for $\mathbf{A}''(t)$ and $\mathbf{a}''(t)$, we obtain that $T_{\mathbf{R}''\mathbf{p}''i}(n) = e^{i(n\omega - U_p)T/2} T_{\mathbf{R}\mathbf{p}i}(n)$, so that $w_{\mathbf{R}''\mathbf{p}''i}(n) = w_{\mathbf{R}\mathbf{p}i}(n)$; i.e., the differential ionization rate is invariant with respect to the transformation

$$\begin{aligned} \theta &\rightarrow -\theta, & \theta_L &\rightarrow 180^\circ - \theta_L, \\ \theta_e &\rightarrow 180^\circ - \theta_e, & r \text{ odd, } s \text{ even.} \end{aligned} \quad (16)$$

Figure 4 shows the HATI spectra obtained by the $\omega-2\omega$ OTC laser field for $\theta_L = 30^\circ$ (left panel) and $\theta_L = 150^\circ$ (right panel). The spectrum calculated for $\theta_L = 30^\circ$ is the mirror image of the spectrum calculated for $\theta_L = 150^\circ$, in accordance with the transformation (16).

Let us consider the case where s is odd and r is even. In this case, the vector quantities describing the laser field are transformed in accordance with the relation (14) and we use the notation with the triple primes, $\mathbf{p}''' = P_{x_L}\mathbf{p}$, etc.,

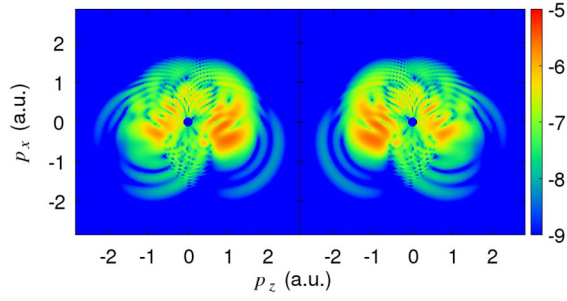


FIG. 4. Logarithm of the differential ionization rate of the N_2 molecule presented in false colors in the photoelectron momentum plane for the case of ionization by the $\omega-2\omega$ OTC laser field having the relative phase $\varphi = 30^\circ$. Molecular orientation angles are $\theta_L = 30^\circ$ (left panel) and $\theta_L = 150^\circ$ (right panel). The results are obtained by using the IMSFA. Other parameters are the same as in Fig. 3.

for the vectors obtained by the reflection with respect to the $y_L z_L$ plane. It can be shown that $w_{\mathbf{R}^m \mathbf{p}^{m'}}(n) = w_{\mathbf{R} \mathbf{p}^i}(n)$, so that the differential ionization rate is invariant under the transformation

$$\theta \rightarrow -\theta, \quad \theta_L \rightarrow -\theta_L, \quad \theta_e \rightarrow -\theta_e, \quad r \text{ even}, \quad s \text{ odd}. \quad (17)$$

This result is illustrated in Fig. 5 where the HATI spectra obtained by the $2\omega-3\omega$ OTC laser field for $\theta_L = -45^\circ$ (upper panel) and $\theta_L = 45^\circ$ (lower panel) are presented. The spectrum calculated for $\theta_L = 45^\circ$ is the mirror image of the spectrum calculated for $\theta_L = -45^\circ$, in accordance with

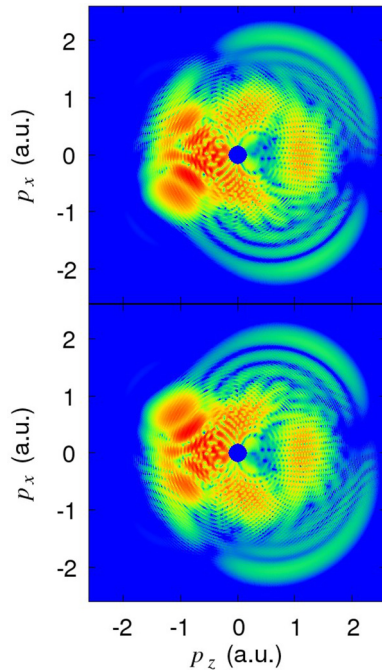


FIG. 5. Logarithm of the differential ionization rate of the N_2 molecule presented in false colors in the photoelectron momentum plane for the case of ionization by the $2\omega-3\omega$ OTC laser field having the relative phase $\varphi = 0^\circ$. Molecular orientation angles are $\theta_L = -45^\circ$ (upper panel) and $\theta_L = 45^\circ$ (lower panel). The results are obtained by using the IMSFA. Other parameters are the same as in Fig. 3.

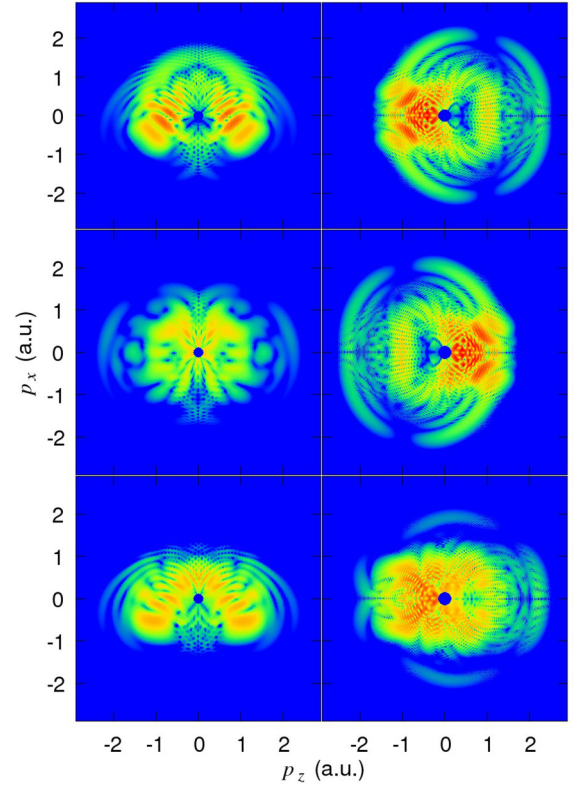


FIG. 6. The same as in Fig. 3 but for the $\omega-2\omega$ (left column) and $2\omega-3\omega$ (right column) OTC laser fields and for the following molecular orientations θ_L and relative phases φ : $\theta_L = 0^\circ$ and $\varphi = 0^\circ$ (top row), $\theta_L = 0^\circ$ and $\varphi = 90^\circ$ (middle row), and $\theta_L = 90^\circ$ and $\varphi = 30^\circ$ (bottom row).

the transformation (17). In addition, as the relation (11) is valid, the spectrum for $\theta_L = -45^\circ$ is identical to the spectrum for $\theta_L = 135^\circ$. Let us now consider special cases. The reflection symmetries of the HATI spectra for the N_2 molecule and molecular orientations $\theta_L = 0^\circ$ and 90° are illustrated in Fig. 6, where the results for the $\omega-2\omega$ (left panels) and $2\omega-3\omega$ (right panels) OTC laser fields are presented. For a homonuclear diatomic molecule the orientations $\theta_L = 0^\circ, 90^\circ$ are left virtually unchanged by the reflections P_{x_L} and P_{z_L} , so that the corresponding HATI spectra obey specific reflection symmetries. For the $\omega-2\omega$ field (s even) the reflection symmetry of each spectra about the p_x axis is valid, while for the $2\omega-3\omega$ field (r even) the reflection symmetry of each spectra about the p_z axis is valid.

Finally, we mention that if $\varphi = 0^\circ$, the interchange of r and s corresponds to the interchange of the z_L and x_L axes. For the atomic HATI spectra obtained by the OTC field, this simply leads to the interchange of the p_z and p_x axes. In the case of HATI of oriented molecules driven by the OTC field, one should keep in mind that the angle of molecular orientation is also transformed with the interchange of the z_L and x_L axes.

3. Direct ATI for the relative phase $\varphi = 90^\circ$

The case of the relative phase $\varphi = 90^\circ$ is specific and requires an additional elaboration. In Fig. 1 the vector-potential (and the electric-field-vector) Lissajous figures are presented

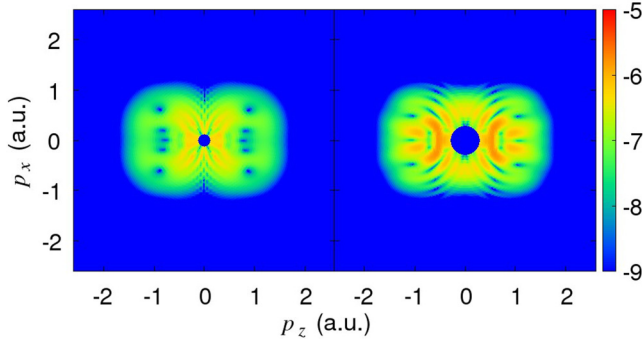


FIG. 7. Logarithm of the differential ionization rate of the N_2 molecule presented in false colors in the photoelectron momentum plane for the case of ionization by the $\omega-2\omega$ (left panel) and $\omega-3\omega$ (right panel) OTC laser fields having the relative phase $\varphi = 90^\circ$. Only the contribution of direct electrons is taken into account. The molecular orientation angle is $\theta_L = 90^\circ$. Other parameters are the same as in Fig. 3.

for $\varphi = 90^\circ$ and for three different OTC fields (i.e., three different combinations of r and s). The Lissajous figures of the vector potential $\mathbf{A}(t)$ for the $\omega-2\omega$ and $\omega-3\omega$ cases obey the reflection symmetry with respect to the x_L and z_L axes. As the pattern of the ATI momentum spectrum (direct photoelectrons only) is strongly related to the vector potential $\mathbf{A}(t)$ contour, it is worth checking whether the same reflection symmetries are valid for the ATI momentum spectrum calculated for $\theta_L = 0^\circ, 90^\circ$. It is easy to show that $P_{x_L}\mathbf{E}(t) = -\mathbf{E}(-t)$, $P_{x_L}\mathbf{A}(t) = -\mathbf{A}(-t)$, and $P_{x_L}\boldsymbol{\alpha}(t) = -\boldsymbol{\alpha}(-t)$ for the laser field (1) if $\varphi = 90^\circ$. This leads to the invariance of the direct photoelectron (ATI) spectrum with respect to the reflection about the p_z axis (see Appendix C in [55]). However, this invariance is absent for the corresponding HATI spectrum. This is due to the fact that the direct ionization is an adiabatic process [54] which depends only on the time of ionization, while the rescattering process is nonadiabatic. The reflection symmetry with respect to the p_x axis is valid if $r + s$ and r are odd, while the C_2 symmetry is valid if $r + s$ is even. It is also easy to prove that the C_2 symmetry, combined with the reflection symmetry about the p_z axis, leads to the reflection symmetry about the p_x axis. Summarizing the above discussion, one can conclude that the direct photoelectron momentum spectrum is invariant under the reflection about the p_x and p_z axes if r is odd, $\varphi = 90^\circ$, and $\theta_L = 0^\circ, 90^\circ$. This is illustrated in Fig. 7, where the direct photoelectron momentum spectra of the N_2 molecule are presented for the $\omega-2\omega$ (left panel) and $\omega-3\omega$ (right panel) OTC laser fields. The angle of molecular orientation and the relative phase are $\theta_L = 90^\circ$ and $\varphi = 90^\circ$, respectively. The ATI spectra in Fig. 7 are invariant under the reflection about the p_x and p_z axes. If $\varphi = 270^\circ$, the obtained spectra have the same symmetry properties as in the case of $\varphi = 90^\circ$.

The symmetries of the direct photoelectron spectra can be violated in some cases, as reported for an elliptically polarized laser field [70,71] and bicircular laser field [53,72]. The zeroth-order term of the MSFA, Eq. (7), gives the main contribution to the low-energy spectra (it decreases exponentially for higher energies). We have shown that these spectra for the

OTC field with the relative phase equal to 90 degrees possess additional symmetries (the reflection symmetries with respect to the p_x and p_z axes; see Fig. 7). These symmetries are violated if the higher-order terms of the MSFA are taken into account or if the Coulomb effects are accounted for (solving, for example, the time-dependent Schrödinger equation).

C. Shift of the relative phase by 180°

In this subsection we compare the HATI spectra obtained with the field (1) for the relative phases φ and $\varphi + 180^\circ$. If the relative phase is changed from φ to $\varphi + 180^\circ$, the x_L component of the vectors $\mathbf{E}(t)$, $\mathbf{A}(t)$, and $\boldsymbol{\alpha}(t)$ changes the sign, so that $\mathbf{E}(t, \varphi + 180^\circ) = P_{x_L}\mathbf{E}(t, \varphi)$ and analogously for $\mathbf{A}(t, \varphi)$ and $\boldsymbol{\alpha}(t, \varphi)$ [for an easier understanding we added the dependence on φ in $\mathbf{E}(t)$]. We are going to consider whether this reflection of the field about the z_L axis simply leads to the reflection of the corresponding molecular HATI spectra about the p_z axis, as it would in the atomic case.

We first analyze the consequences of this relative-phase shift in the case when r is odd and s even. According to (13), the following relation is valid:

$$\mathbf{E}(t + T/2, \varphi + 180^\circ) = R_y(\pi)\mathbf{E}(t, \varphi), \quad r \text{ odd, } s \text{ even,} \quad (18)$$

where we used the relation $P_{x_L}P_{z_L} = R_y(\pi)$. Since the laser field is periodic, the differential ionization rate (3) remains unchanged if the time shift is applied in relation (4). The homonuclear diatomic molecules are invariant with respect to the rotation $R_y(\pi)$, so that it is clear that the relative-phase shift $\varphi \rightarrow \varphi + 180^\circ$ leads to the rotation of the entire photoelectron momentum spectrum by the angle 180° with respect to the p_y axis. This is illustrated in the top panels of Fig. 8, where the HATI spectra of the N_2 molecule in the $\omega-2\omega$ OTC laser field are presented for $\varphi = 30^\circ$ (top left panel) and $\varphi = 210^\circ$ (top right panel), with $\theta_L = 45^\circ$. Next, we analyze the case where r is even and s is odd. Using (14) and the relation $P_{x_L}^2 = 1$, we obtain

$$\mathbf{E}(t + T/2, \varphi + 180^\circ) = \mathbf{E}(t, \varphi), \quad r \text{ even, } s \text{ odd.} \quad (19)$$

In this case, the phase shift $\varphi \rightarrow \varphi + 180^\circ$ leaves the HATI spectrum unchanged. An example is illustrated in Fig. 9, where the HATI photoelectron momentum spectra of the N_2 molecule are presented for the $2\omega-3\omega$ OTC laser field having the relative phases $\varphi = 30^\circ, 210^\circ$. The spectra obtained with $\varphi = 30^\circ$ and $\varphi = 210^\circ$ are identical.

If both r and s are odd, the time-shift transformation of $\mathbf{E}(t)$ is given by (12). In this case we have

$$\mathbf{E}(t + T/2, \varphi + 180^\circ) = P_{z_L}\mathbf{E}(t, \varphi), \quad r, s \text{ both odd,} \quad (20)$$

where we used the relation $P_{x_L}R_y(\pi) = P_{z_L}$. For the HATI of atoms, Eq. (20) leads to the symmetry transformation $w_{\mathbf{p}}(\varphi) = w_{\mathbf{p}''}(\varphi + 180^\circ)$, with $\mathbf{p}'' = P_{z_L}\mathbf{p}$. However, this relation is not generally valid in the molecular case. The absence of this symmetry is illustrated in the middle panels of Fig. 8, where the HATI photoelectron momentum spectra of the N_2 molecule in the $\omega-3\omega$ OTC laser field are presented. The angle of molecular orientation is $\theta_L = 45^\circ$, while the relative phases are $\varphi = 30^\circ$ (middle left panel) and $\varphi = 210^\circ$ (middle right panel). There is no symmetry transformation that relates the two spectra in the middle panels of Fig. 8. This can be

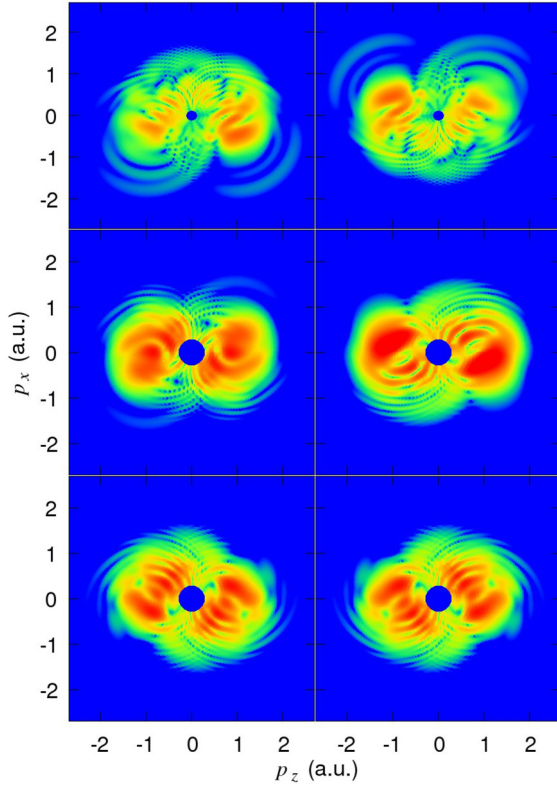


FIG. 8. Same as in Fig. 3 but for the $\omega-2\omega$ (top row) and $\omega-3\omega$ (middle and bottom rows) OTC laser fields. The results calculated for the relative phases $\varphi = 30^\circ$ and $\varphi = 210^\circ$ are presented in the left column and the right column, respectively. The molecular orientation angle is $\theta_L = 45^\circ$ (top and middle rows) and $\theta_L = 0^\circ$ (bottom row).

explained by the fact that an oriented homonuclear diatomic molecule generally does not obey the same symmetry transformation as the laser field, with the exception of the molecule aligned along the z_L axis or along the x_L axis. In the case of an arbitrarily oriented molecule, the symmetry transformation of the spectra is $w_{\mathbf{R}\mathbf{p}_i}(\varphi) = w_{\mathbf{R}'\mathbf{p}'_i}(\varphi + 180^\circ)$. This can be illustrated by comparing the HATI spectrum obtained for $\theta_L = 135^\circ$ and $\varphi = 30^\circ$ (middle left panel of Fig. 3) with the one obtained for $\theta_L = 45^\circ$ and $\varphi = 210^\circ$ (middle right panel of Fig. 8). These two spectra are mirror images of each other. It is worth noticing that the reflections with respect to the p_z and p_x axes give the same result if the diatomic molecule is homonuclear and $r + s$ is even, since the C_2 symmetry of the HATI spectra is valid in this case. For $\mathbf{R} = \pm R\hat{\mathbf{e}}_{z_L}$ or $\pm R\hat{\mathbf{e}}_{x_L}$ ($\theta_L = 0^\circ, 180^\circ$, or $\pm 90^\circ$) the reflection with respect to the p_z axis leaves the molecular orientation (virtually) unchanged and the symmetry transformation is $w_{\mathbf{R}\mathbf{p}_i}(\varphi) = w_{\mathbf{R}\mathbf{p}'_i}(\varphi + 180^\circ)$. This is illustrated in the bottom panels of Fig. 8, where the HATI spectra of the N_2 molecule in the $\omega-3\omega$ OTC laser field are presented. The molecular orientation angle is $\theta_L = 0^\circ$, while the relative phases are $\varphi = 30^\circ$ (bottom left panel) and $\varphi = 210^\circ$ (bottom right panel).

IV. DESTRUCTIVE INTERFERENCE MINIMA

In this section we will show that the destructive interference minima can be observed in the spectra of electrons

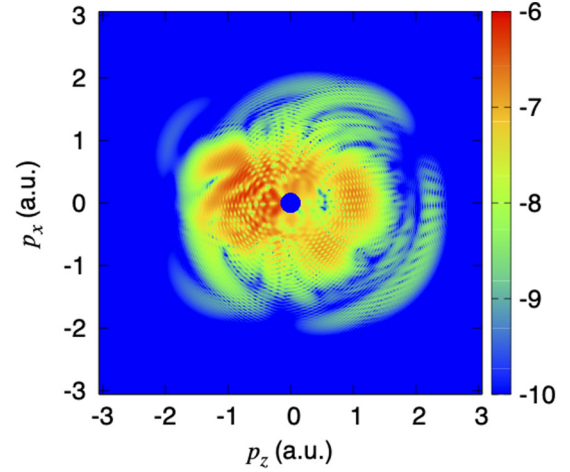


FIG. 9. Logarithm of the differential ionization rate of the N_2 molecule presented in false colors in the photoelectron momentum plane for the case of ionization by the $2\omega-3\omega$ OTC laser field. The molecular orientation angle is $\theta_L = 30^\circ$. The presented spectrum corresponds to the relative phases $\varphi = 30^\circ, 210^\circ$. Other parameters are the same as in Fig. 3.

liberated in ionization of a diatomic molecule by an OTC field and that the position of these minima is in accordance with the condition (10) which we derived using our IMSFA theory. For the parameters used in our paper only the lowest-order ($m = 0$) destructive interference condition can be achieved. Taking also into account that $p_z = p \cos \theta_e$ and $p_x = p \sin \theta_e$, for $\theta_e = 0$, i.e., for the electrons emitted in the direction of the ω OTC field component, Eq. (10) can be rewritten as

$$[(p - k_{z,\text{st}}) \cos \theta_L + k_{x,\text{st}} \sin \theta_L]^2 = \pi^2 / R^2. \quad (21)$$

For fixed laser parameters and internuclear distance the above equation is a nonlinear equation which connects the photoelectron energy $E_p = p^2/2$ and the molecular orientation angle θ_L . Solution of this equation determines a curve in the (θ_L, E_p) plane.

The stationary momentum $\mathbf{k}_{\text{st}} = -[\boldsymbol{\alpha}(t) - \boldsymbol{\alpha}(t_0)]/(t - t_0)$ can be determined using the quantum-orbit theory and the saddle-point method [6,73]. In short, the condition that the action, which appears in the exponent of the subintegral function (integral is over the ionization time t_0 and the rescattering time t), is stationary leads to the system of equations $[\mathbf{k}_{\text{st}} + \mathbf{A}(t_0)]^2 = -2I_p$ and $[\mathbf{p} + \mathbf{A}(t)]^2 = [\mathbf{k}_{\text{st}} + \mathbf{A}(t)]^2$, which should be solved over t_0 and t . For the OTC field the corresponding solutions can be found in [74]. For example, for the $\omega-2\omega$ OTC field with the relative phase $\varphi = 180^\circ$, the dominant quantum orbit which is responsible for the high-energy plateau corresponds to $t_0 \approx -0.13T$ and $t \approx 0.48T$ (solutions t_0 and t are complex but for our purpose we take only their real parts). Using this result we calculate the corresponding values of $k_{z,\text{st}}$ and $k_{x,\text{st}}$ and introduce them into Eq. (21). For the relative phase $\varphi = 90^\circ$ two quantum orbits are dominant, the shorter one in the high-energy region ($t_0 \approx -0.24T$ and $t \approx 0.55T$) and the longer one in the intermediate energy region ($t_0 \approx -0.73T$ and $t \approx 0.57T$).

In Fig. 10 we present the logarithm of the differential ionization rate in false colors in the (θ_L, E_p) plane. Ionization

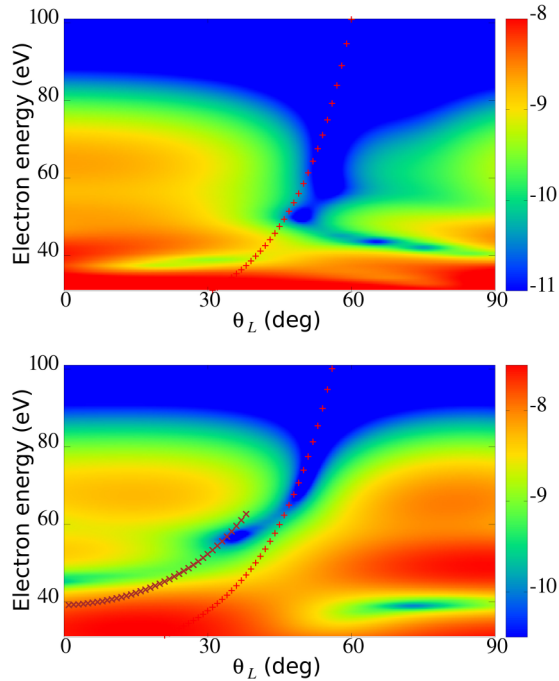


FIG. 10. Logarithm of the differential ionization rate of the N_2 molecule presented in false colors in the molecular orientation angle–photoelectron energy plane. The ionization is by the ω – 2ω OTC laser field having the wavelength 800 nm and intensity of the laser-field components $I = 1.2 \times 10^{14}$ W/cm². The electrons are emitted in the direction $\theta_e = 0$. The presented spectra correspond to the relative phases $\varphi = 180^\circ$ (upper panel) and $\varphi = 90^\circ$ (lower panel). The curves which satisfy the destructive interference condition (21) are presented by the symbols “ \times ” and “+”, as explained in the text. The false-color scale cover three orders of magnitude.

of the N_2 molecule is by the ω – 2ω OTC laser field and the electrons are emitted in the direction $\theta_e = 0$. For the chosen relative phases we calculate the stationary momentum \mathbf{k}_{st} using the saddle-point method, as described above. Introducing this result into the destructive interference condition (21) we obtain a curve in the (θ_L, E_p) plane. This curve is depicted in Fig. 10 for the relative phase $\varphi = 180^\circ$ in the upper panel and for $\varphi = 90^\circ$ in the lower panel. For the phase $\varphi = 180^\circ$ only one saddle-point solution is dominant for the high electron energies and the corresponding curve is depicted by the symbol “+” in the upper panel of Fig. 10. One can see that this curve fits well the interference minima in the numerically calculated differential ionization rate. For the phase $\varphi = 90^\circ$ two destructive interference curves are shown in the lower panel of Fig. 10. The curve denoted by the symbol “+” corresponds to shorter orbits and higher energies, while the curve denoted by the symbol “ \times ” corresponds to longer orbits having lower energies (and shorter plateau and cutoff). The presented curves again fit well numerically calculated minima. This confirms our theory and the predictive power of the simple analytical destructive interference condition we derived.

It was recently demonstrated [65] that the destructive interference minima in the form of a valley structure appear in the two-dimensional photoelectron spectra in ATI experiments

with aligned diatomic molecules exposed to a linearly polarized field. Based on this, in [65] a tomographic method to extract the molecular internuclear separation was demonstrated for the first time and it was claimed that this method provides a more straightforward approach of molecular imaging, in comparison with, e.g., laser-induced electron diffraction and fixed-angle broadband laser-driven electron scattering. We have shown here that such interference minima appear also for the OTC field. In Fig. 10 the energy is in electronvolts (the corresponding ponderomotive energy is $1U_p = 8.96$ eV), as in Fig. 2 in [65]. The OTC field is two-dimensional (i.e., it develops in a plane, in comparison with the one-dimensional linearly polarized laser field). Having also in mind that the OTC laser field provides an easily experimentally controllable parameter, the relative phase between the laser-field components, we hope that the results presented in our paper will help experimentalists to improve their tomographic method.

V. CONCLUSIONS AND COMMENTS

We have applied the improved molecular strong-field approximation to investigate the photoelectron distributions for high-order above-threshold ionization of homonuclear diatomic molecules by an orthogonally polarized two-color laser field having the component frequencies $r\omega$ and $s\omega$ and the relative phase φ . The contributions of both the direct and rescattered electrons to the photoelectron momentum spectra are taken into account. We have considered the case of homonuclear diatomic molecules aligned in the laser-field polarization plane. Two rotational and two reflection symmetries have been found which are valid for arbitrary values of the relative phase.

Two rotational symmetries of the HATI spectra are valid for every molecular orientation. The first rotational symmetry is the C_2 symmetry that is valid for the molecular HATI photoelectron spectrum if the integer multiples r and s of the fundamental laser frequency are both odd, Eq. (15). The second rotational symmetry refers to the rotational transformation of the HATI spectra in the case of the relative-phase shift $\varphi \rightarrow \varphi + 180^\circ$ if $r + s$ is odd. If r is odd, the above-mentioned phase shift leads to the HATI spectra transformation $\theta_e \rightarrow \theta_e + 180^\circ$ [see Eq. (18) and the top panels of Fig. 8]. If r is even, the HATI spectra are invariant with respect to the $\varphi \rightarrow \varphi + 180^\circ$ phase shift [see Eq. (19)].

The first reflection symmetry is valid for the HATI spectra if $r + s$ is odd. It is the reflection with respect to the p_x (p_z) axis if s (r) is even, presented with the relation (16) [(17)], so that the HATI spectrum, obtained for an arbitrary orientation angle θ_L , is the mirror image of the corresponding HATI spectrum obtained for the orientation angle $180^\circ - \theta_L$ ($-\theta_L$). Specifically, for the orientations $\theta_L = 0^\circ, \pm 90^\circ, 180^\circ$ the corresponding HATI spectrum obeys the reflection symmetry about the p_x (p_z) axis when s (r) is even. The second reflection symmetry is related to the transformation of the HATI spectra for the relative-phase shift $\varphi \rightarrow \varphi + 180^\circ$ if r and s are both odd, Eq. (20). Regarding these reflection symmetries, the HATI spectrum obtained for an arbitrary angle θ_L is the mirror image of the corresponding HATI spectrum obtained for the angle $180^\circ - \theta_L$ (compare the spectrum presented in the middle left panel of Fig. 3 with the spectrum presented in the

middle right panel of Fig. 8). Specifically, for the orientations $\theta_L = 0^\circ, \pm 90^\circ, 180^\circ$ this phase-shift transformation results in the HATI spectra transformation $\theta_e \rightarrow -\theta_e$.

The above-described symmetries are a consequence of the dynamical symmetry transformations of the OTC field (1) and of the rotational (C_2) and reflection symmetries of the homonuclear diatomic molecules. They are all valid for both the direct and the rescattered electrons, and beyond the IMSFA formalism. We illustrated our results with the examples of the HATI spectra of the N_2 molecule for various combinations of the laser-field-component frequencies and for various values of the relative phase and of the molecular orientation angle. The obtained results are independent of the relative intensity of the OTC field components.

In addition to the symmetries of the HATI spectra, we have found reflection symmetries which are valid only for the direct ATI spectra (the departures from these symmetries due to the contribution of the nonadiabatic HATI process are barely visible when presented on a linear scale). These are reflection symmetries with respect to the p_x and p_z axes for r odd, $\varphi = 90^\circ$, and $\theta_L = 0^\circ, 90^\circ$ (see Sec. III B 3). We have illustrated this in Fig. 7.

We expect that our results for HATI by the OTC field are reliable, except maybe in the low-energy region where the Coulomb effects are important. This conclusion is supported by the results of Ref. [75] where HATI of the H_2^+ ion by a linearly polarized laser field was investigated using numerical solutions of the full three-dimensional TDSE. In [75] it was shown that the predictions of the quantum-orbit theory (which is an approximation to our IMSFA theory) agree

very well with these TDSE results. We also expect that the symmetries discovered in our paper can be applied to test the theoretical results obtained using more sophisticated methods. As concerns the time-consuming TDSE calculations, these symmetries can be used to control their quality and robustness as well as to decrease the computation time (having in mind that the symmetries are violated for few-cycle laser pulses [66]).

We have derived an analytical formula for the position of the destructive interference minima which we have observed in our numerical results for the yield of the photoelectrons emitted in the direction of the ω OTC field component, presented in false colors in the molecular orientation angle–photoelectron energy plane. The appearance and the position of these minima are determined by the internuclear distance R and the laser-field parameters. Our analytical formula fits well the results obtained by numerical integration. Since, in comparison with a linearly polarized laser field, our OTC field develops in a plane and since we have an additional control parameter, the relative phase between the laser-field components, a possible application of our results is to improve the method of tomographic extraction of the internuclear separation, demonstrated in [65] using a linearly polarized laser field.

ACKNOWLEDGMENTS

We gratefully acknowledge support by the Ministry for Education, Science, and Youth, Canton Sarajevo, Bosnia and Herzegovina.

-
- [1] P. B. Corkum, Plasma Perspective on Strong Field Multiphoton Ionization, *Phys. Rev. Lett.* **71**, 1994 (1993).
 - [2] K. C. Kulander, K. J. Schafer, and J. L. Krause, Dynamics of short-pulse excitation, ionization and harmonic conversion, in *Super-Intense Laser-Atom Physics*, edited by B. Piraux, A. L’Huillier, and K. Rzażewski, NATO Advanced Studies Institute, Series B: Physics Vol. 316 (Plenum, New York, 1993), p. 95.
 - [3] M. Lewenstein, Ph. Balcou, M. Yu. Ivanov, A. L’Huillier, and P. B. Corkum, Theory of high-harmonic generation by low-frequency laser fields, *Phys. Rev. A* **49**, 2117 (1994).
 - [4] G. G. Paulus, W. Becker, W. Nicklich, and H. Walther, Rescattering effects in above-threshold ionization: A classical model, *J. Phys. B* **27**, L703 (1994).
 - [5] P. Agostini, F. Fabre, G. Mainfray, G. Petite, and N. K. Rahman, Free-Free Transitions Following Six-Photon Ionization of Xenon Atoms, *Phys. Rev. Lett.* **42**, 1127 (1979).
 - [6] W. Becker, F. Grasbon, R. Kopold, D. B. Milošević, G. G. Paulus, and H. Walther, Above-threshold ionization: From classical features to quantum effects, *Adv. At. Mol. Opt. Phys.* **48**, 35 (2002).
 - [7] W. Becker, S. P. Goreslavski, G. G. Paulus, and D. B. Milošević, The plateau in above-threshold ionization: The keystone of rescattering physics, *J. Phys. B* **51**, 162002 (2018).
 - [8] M. Lein and M. Wollenhaupt, Special issue: Dynamics in tailored ultrashort light fields, *J. Mod. Opt.* **64**, 949 (2018).
 - [9] H. Eichmann, A. Egbert, S. Nolte, C. Momma, B. Wellegehausen, W. Becker, S. Long and J. K. McIver, Polarization-dependent high-order two-color mixing, *Phys. Rev. A* **51**, R3414 (1995).
 - [10] S. Long, W. Becker, and J. K. McIver, Model calculations of polarization-dependent two-color high-harmonic generation, *Phys. Rev. A* **52**, 2262 (1995).
 - [11] D. B. Milošević, W. Becker, and R. Kopold, Generation of circularly polarized high-order harmonics by two-color coplanar field mixing, *Phys. Rev. A* **61**, 063403 (2000).
 - [12] A. Fleischer, O. Kfir, T. Diskin, P. Sidorenko, and O. Cohen, Spin angular momentum and tunable polarization in high-harmonic generation, *Nat. Photonics* **8**, 543 (2014).
 - [13] A. D. Bandrauk, J. Guo, and K.-J. Yuan, Circularly polarized attosecond pulse generation and applications to ultrafast magnetism, *J. Opt.* **19**, 124016 (2017).
 - [14] D. B. Milošević and W. Becker, X-ray harmonic generation by orthogonally polarized two-color fields: Spectral shape and polarization, *Phys. Rev. A* **100**, 031401(R) (2019).
 - [15] M. Kitzler and M. Lezius, Spatial Control of Recollision Wave Packets with Attosecond Precision, *Phys. Rev. Lett.* **95**, 253001 (2005).
 - [16] M. Kitzler, K. O’Keeffe and M. Lezius, Attosecond control of electronic motion using light wave synthesis, *J. Mod. Opt.* **53**, 57 (2006).

- [17] Y. Zhou, C. Huang, Q. Liao, W. Hong, and P. Lu, Control the revisit time of the electron wave packet, *Opt. Lett.* **36**, 2758 (2011).
- [18] X. Xie, Two-Dimensional Attosecond Electron Wave-Packet Interferometry, *Phys. Rev. Lett.* **114**, 173003 (2015).
- [19] D. Würzler, N. Eicke, M. Möller, D. Seipt, A. M. Saylor, S. Fritzsche, M. Lein, and G. G. Paulus, Velocity map imaging of scattering dynamics in orthogonal two-color fields, *J. Phys. B* **51**, 015001 (2018).
- [20] D. Shafir, H. Soifer, B. D. Bruner, M. Dagan, Y. Mairesse, S. Patchkovskii, M. Yu. Ivanov, O. Smirnova, and N. Dudovich, Resolving the time when an electron exits a tunnelling barrier, *Nature (London)* **485**, 343 (2012).
- [21] J.-H. Chen, M. Han, X.-R. Xiao, L.-Y. Peng, and Y. Liu, Atomic-orbital-dependent photoelectron momentum distributions for F^- ions by orthogonal two-color laser fields, *Phys. Rev. A* **98**, 033403 (2018).
- [22] M. Li, J.-W. Geng, M.-M. Liu, X. Zheng, L.-Y. Peng, Q. Gong, and Y. Liu, Spatial-temporal control of interferences of multiple tunneling photoelectron wave packets, *Phys. Rev. A* **92**, 013416 (2015).
- [23] J.-W. Geng, W.-H. Xiong, X.-R. Xiao, L.-Y. Peng, and Q. Gong, Nonadiabatic Electron Dynamics in Orthogonal Two-Color Laser Fields with Comparable Intensities, *Phys. Rev. Lett.* **115**, 193001 (2015).
- [24] J. Henkel and M. Lein, Analysis of electron trajectories with two-color strong-field ionization, *Phys. Rev. A* **92**, 013422 (2015).
- [25] M. He, Y. Li, Y. Zhou, M. Li, and P. Lu, Temporal and spatial manipulation of the recolliding wave packet in strong-field photoelectron holography, *Phys. Rev. A* **93**, 033406 (2016).
- [26] N. Eicke and M. Lein, Extracting trajectory information from two-color strong-field ionization, *J. Mod. Opt.* **64**, 981 (2017).
- [27] Y. Li, Y. Zhou, M. He, M. Li, and P. Lu, Identifying backward-rescattering photoelectron hologram with orthogonal two-color laser fields, *Opt. Express* **24**, 23697 (2016).
- [28] X. Gong, C. Lin, F. He, Q. Song, K. Lin, Q. Ji, W. Zhang, J. Ma, P. Lu, Y. Liu, H. Zeng, W. Yang, and J. Wu, Energy-Resolved Ultrashort Delays of Photoelectron Emission Clocked by Orthogonal Two-Color Laser Fields, *Phys. Rev. Lett.* **118**, 143203 (2017).
- [29] M. Han, P. Ge, Y. Shao, M.-M. Liu, Y. Deng, C. Wu, Q. Gong, and Y. Liu, Revealing the Sub-Barrier Phase using a Spatiotemporal Interferometer with Orthogonal Two-Color Laser Fields of Comparable Intensity, *Phys. Rev. Lett.* **119**, 073201 (2017).
- [30] X. Xie, T. Wang, S. G. Yu, X. Y. Lai, S. Roither, D. Kartashov, A. Baltuška, X. J. Liu, A. Staudte, and M. Kitzler, Disentangling Intracycle Interferences in Photoelectron Momentum Distributions Using Orthogonal Two-Color Laser Fields, *Phys. Rev. Lett.* **119**, 243201 (2017).
- [31] J. Tan, Y. Zhou, M. He, Y. Chen, Q. Ke, J. Liang, X. Zhu, M. Li, and P. Lu, Determination of the Ionization Time Using Attosecond Photoelectron Interferometry, *Phys. Rev. Lett.* **121**, 253203 (2018).
- [32] J. Tan, Y. Zhou, M. He, Q. Ke, J. Liang, Y. Li, M. Li, and P. Lu, Time-resolving tunneling ionization via strong-field photoelectron holography, *Phys. Rev. A* **99**, 033402 (2019).
- [33] W. Xie, M. Li, S. Luo, M. He, K. Liu, Q. Zhang, Y. Zhou, and P. Lu, Nonadiabaticity-induced ionization time shift in strong-field tunneling ionization, *Phys. Rev. A* **100**, 023414 (2019).
- [34] M. Li, H. Xie, W. Cao, S. Luo, J. Tan, Y. Feng, B. Du, W. Zhang, Y. Li, Q. Zhang, P. Lan, Y. Zhou, and P. Lu, Photoelectron Holographic Interferometry to Probe the Longitudinal Momentum Offset at the Tunnel Exit, *Phys. Rev. Lett.* **122**, 183202 (2019).
- [35] M. Han, P. Ge, Y. Fang, Y. Deng, C. Wu, Q. Gong, and Y. Liu, Quantum effect of laser-induced rescattering from the tunneling barrier, *Phys. Rev. A* **99**, 023418 (2019).
- [36] F. Jin, H. Yang, B. Wang, L. Wei, and H. Wu, Angular resolved above-threshold ionization spectrum of an atom in IR+XUV orthogonally polarized two-color laser fields, *Opt. Express* **27**, 20754 (2019).
- [37] Y. Liu, J. Tan, M. He, H. Xie, Y. Qin, Y. Zhao, M. Li, Y. Zhou, and P. Lu, Photoelectron holographic interferences from multiple returning in strong-field tunneling ionization, *Opt. Quantum Electron.* **51**, 145 (2019).
- [38] N. Eicke, S. Brennecke, and M. Lein, Attosecond-Scale Streaking Methods for Strong-Field Ionization by Tailored Fields, *Phys. Rev. Lett.* **124**, 043202 (2020).
- [39] F. Lindner, M. G. Schätzel, H. Walther, A. Baltuška, E. Goulielmakis, F. Krausz, D. B. Milošević, D. Bauer, W. Becker, and G. G. Paulus, Attosecond Double-Slit Experiment, *Phys. Rev. Lett.* **95**, 040401 (2005).
- [40] M. Richter, M. Kunitski, M. Schöffler, T. Jahnke, L. P. H. Schmidt, M. Li, Y. Liu, and R. Dörner, Streaking Temporal Double-Slit Interference by an Orthogonal Two-Color Laser Field, *Phys. Rev. Lett.* **114**, 143001 (2015).
- [41] D. B. Milošević, Possibility of introducing spin into attoscience with spin-polarized electrons produced by a bichromatic circularly polarized laser field, *Phys. Rev. A* **93**, 051402(R) (2016).
- [42] M. Han, P. Ge, M.-M. Liu, Q. Gong, and Y. Liu, Spatially and temporally controlling electron spin polarization in strong-field ionization using orthogonal two-color laser fields, *Phys. Rev. A* **99**, 023404 (2019).
- [43] K.-J. Yuan, S. Chelkowski, and A. D. Bandrauk, Molecular photoelectron momentum distributions by intense orthogonally polarized attosecond ultraviolet laser pulses, *Chem. Phys. Lett.* **638**, 173 (2015).
- [44] F. Gao, Y. J. Chen, G. G. Xin, J. Liu and L. B. Fu, Distilling two-center-interference information during tunneling of aligned molecules with orthogonally polarized two-color laser fields, *Phys. Rev. A* **96**, 063414 (2017).
- [45] M.-M. Liu, M. Han, P. Ge, C. He, Q. Gong, and Y. Liu, Strong-field ionization of diatomic molecules in orthogonally polarized two-color fields, *Phys. Rev. A* **97**, 063416 (2018).
- [46] X. Gong, P. He, Q. Song, Q. Ji, H. Pan, J. Ding, F. He, H. Zeng, and J. Wu, Two-Dimensional Directional Proton Emission in Dissociative Ionization of H_2 , *Phys. Rev. Lett.* **113**, 203001 (2014).
- [47] P. V. Demekhin, A. N. Artemyev, A. Kastner, and T. Baumert, Photoelectron Circular Dichroism with Two Overlapping Laser Pulses of Carrier Frequencies ω and 2ω Linearly Polarized in Two Mutually Orthogonal Directions, *Phys. Rev. Lett.* **121**, 253201 (2018).
- [48] J. H. Mun, H. Sakai, and R. González-Férez, Orientation of linear molecules in two-color laser fields with perpendicularly crossed polarizations, *Phys. Rev. A* **99**, 053424 (2019).
- [49] O. Neufeld, D. Podolsky, and O. Cohen, Floquet group theory and its application to selection rules in harmonic generation, *Nat. Commun.* **10**, 405 (2019).

- [50] X. Liu, X. Zhu, L. Li, Y. Li, Q. Zhang, P. Lan, and P. Lu, Selection rules of high-order-harmonic generation: Symmetries of molecules and laser fields, *Phys. Rev. A* **94**, 033410 (2016).
- [51] D. B. Milošević, Circularly polarized high harmonics generated by a bicircular field from inert atomic gases in the p state: A tool for exploring chirality-sensitive processes, *Phys. Rev. A* **92**, 043827 (2015).
- [52] F. Mauger, A. D. Bandrauk, and T. Uzer, Circularly polarized molecular high harmonic generation using a bicircular laser, *J. Phys. B* **49**, 10LT01 (2016).
- [53] D. B. Milošević and W. Becker, Improved strong-field approximation and quantum-orbit theory: Application to ionization by a bicircular laser field, *Phys. Rev. A* **93**, 063418 (2016).
- [54] A. Gazibegović-Busuladžić, W. Becker, and D. B. Milošević, Helicity asymmetry in strong-field ionization of atoms by a bicircular laser field, *Opt. Express* **26**, 12684 (2018).
- [55] M. Busuladžić, A. Gazibegović-Busuladžić, and D. B. Milošević, Strong-field ionization of homonuclear diatomic molecules by a bicircular laser field: Rotational and reflection symmetries, *Phys. Rev. A* **95**, 033411 (2017).
- [56] D. B. Milošević, Strong-field approximation for ionization of a diatomic molecule by a strong laser field, *Phys. Rev. A* **74**, 063404 (2006).
- [57] Z. Ansari, M. Böttcher, B. Manschwetus, H. Rottke, W. Sandner, A. Verhoef, M. Lezius, G. G. Paulus, A. Saenz, and D. B. Milošević, Interference in strong-field ionization of a two-centre atomic system, *New J. Phys.* **10**, 093027 (2008).
- [58] M. Busuladžić and D. B. Milošević, Simulation of the above-threshold-ionization experiment using the molecular strong-field approximation: The choice of gauge, *Phys. Rev. A* **82**, 015401 (2010).
- [59] M. Busuladžić, A. Gazibegović-Busuladžić, D. B. Milošević, and W. Becker, Angle-Resolved High-Order Above-Threshold Ionization of a Molecule: Sensitive Tool for Molecular Characterization, *Phys. Rev. Lett.* **100**, 203003 (2008).
- [60] M. Busuladžić, A. Gazibegović-Busuladžić, D. B. Milošević, and W. Becker, Strong-field approximation for ionization of a diatomic molecule by a strong laser field. II. The role of electron rescattering off the molecular centers, *Phys. Rev. A* **78**, 033412 (2008).
- [61] M. Busuladžić, A. Gazibegović-Busuladžić, and D. B. Milošević, Strong-field approximation for ionization of a diatomic molecule by a strong laser field. III. High-order above-threshold ionization by an elliptically polarized field, *Phys. Rev. A* **80**, 013420 (2009).
- [62] M. Okunishi, R. Itaya, K. Shimada, G. Prümper, K. Ueda, M. Busuladžić, A. Gazibegović-Busuladžić, D. B. Milošević, and W. Becker, Angle-resolved high-order above-threshold ionization spectra for N_2 and O_2 : Measurements and the strong-field approximation, *J. Phys. B* **41**, 201004 (2008).
- [63] M. Okunishi, R. Itaya, K. Shimada, G. Prümper, K. Ueda, M. Busuladžić, A. Gazibegović-Busuladžić, D. B. Milošević, and W. Becker, Two-Source Double-Slit Interference in Angle-Resolved High-Energy Above-Threshold Ionization Spectra of Diatoms, *Phys. Rev. Lett.* **103**, 043001 (2009).
- [64] H. Kang, W. Quan, Y. Wang, Z. Lin, M. Wu, H. Liu, X. Liu, B. B. Wang, H. J. Liu, Y. Q. Gu, X. Y. Jia, J. Liu, J. Chen, and Y. Cheng, Structure Effects in Angle-Resolved High-Order Above-Threshold Ionization of Molecules, *Phys. Rev. Lett.* **104**, 203001 (2010).
- [65] R. P. Sun, X. Y. Lai, S. G. Yu, Y. L. Wang, S. P. Xu, W. Quan, and X. J. Liu, Tomographic Extraction of the Internuclear Separation Based on Two-Center Interference with Aligned Diatomic Molecules, *Phys. Rev. Lett.* **122**, 193202 (2019).
- [66] A. Gazibegović-Busuladžić, E. Hasović, M. Busuladžić, D. B. Milošević, F. Kelkensberg, W. K. Siu, M. J. J. Vrakking, F. Lépine, G. Sansone, M. Nisoli, I. Znakovskaya, and M. F. Kling, Above-threshold ionization of diatomic molecules by few-cycle laser pulses, *Phys. Rev. A* **84**, 043426 (2011).
- [67] W. Quan, X.-Y. Lai, Y.-J. Chen, C.-L. Wang, Z.-L. Hu, X.-J. Liu, X.-L. Hao, J. Chen, E. Hasović, M. Busuladžić, W. Becker, and D. B. Milošević, Resonancelike enhancement in high-order above-threshold ionization of molecules, *Phys. Rev. A* **88**, 021401(R) (2013).
- [68] W. Quan, X.-Y. Lai, Y.-J. Chen, C.-L. Wang, Z.-L. Hu, X. Liu, X.-L. Hao, J. Chen, E. Hasović, M. Busuladžić, D. B. Milošević, and W. Becker, Quantum orbits: A powerful concept in laser-atom physics, *Chin. J. Phys.* **52**, 389 (2014).
- [69] A. Gazibegović-Busuladžić, M. Busuladžić, E. Hasović, W. Becker, and D. B. Milošević, Strong-field ionization of linear molecules by a bicircular laser field: Symmetry considerations, *Phys. Rev. A* **97**, 043432 (2018).
- [70] A. Gazibegović-Busuladžić, D. B. Milošević, and W. Becker, High-energy above-threshold detachment from negative ions, *Phys. Rev. A* **70**, 053403 (2004).
- [71] S. V. Popruzhenko, G. G. Paulus and D. Bauer, Coulomb-corrected quantum trajectories in strong-field ionization, *Phys. Rev. A* **77**, 053409 (2008).
- [72] P. Stammer, S. Patchkovskii, and F. Morales, Evidence of ac-Stark-shifted resonances in intense two-color circularly polarized laser fields, *Phys. Rev. A* **101**, 033405 (2020).
- [73] D. B. Milošević, Strong-field approximation and quantum orbits, in *Computational Strong-Field Quantum Dynamics: Intense Light-Matter Interactions*, edited by D. Bauer (De Gruyter Textbook, Berlin, 2016), Chap. VII, pp. 199–221.
- [74] A. Jašarević, E. Hasović, R. Kopold, W. Becker, and D. B. Milošević, Application of the saddle-point method to strong-laser-field ionization, *J. Phys. A* **53**, 125201 (2020); A. Jašarević, Application of the quantum-orbit method to ionization by an orthogonal bichromatic field (in Bosnian), M.Sc. thesis, University of Sarajevo, 2019.
- [75] B. Fetić and D. B. Milošević, High-order above-threshold ionization of the H_2^+ ion: The role of internuclear distance, *Phys. Rev. A* **99**, 043426 (2019).